JOURNAL OF CATALYSIS **174,** 201–209 (1998)
ARTICLE NO. CA981968

Isomerization of 1-Cyclohexyloctane on Pt/H-ZSM-22 Bifunctional Zeolite Catalyst

W. Souverijns, A. Houvenaghel, E. J. P. Feijen, J. A. Martens, and P. A. Jacobs

Centrum voor Oppervlaktechemie en Katalyse, Departement Interfasechemie, K.U., Leuven, Kard. Mercierlaan 92, B-3001 Heverlee, Belgium
E-mail: johan.martens@agr.kuleuven.ac.be

Received August 1, 1997; revised October 27, 1997; accepted October 27, 1997

1-Cyclohexyloctane is isomerized in the vapor phase on Pt/H-ZSM-22 zeolite catalyst in the presence of hydrogen. Most of the reaction products are identified and analyzed using high-resolution GC and GC/MS. The reaction pathways of 1-cyclohexyloctane are interpreted in terms of alkylcarbenium/alkylcarbonium ion chemistry. The main isomerization pathways are branching of the ring, elongation and shortening of alkyl substituents on the ring, and ring contractions and expansions. A less important pathway is chain branching, occurring selectively at C-atom positions distant from the ring. In the reaction product fraction of heptyl, methylcyclohexanes, preferential formation of the 1-heptyl-*t*-4-methylcyclohexane is observed. The formation of 1-heptyl, 1′-methylcyclohexane is completely suppressed. The peculiar selectivity patterns are explained by a mechanism in which the molecules react in micropore mouths at the external surface of the ZSM-22 zeolite crystals.

INTRODUCTION

Alicyclic hydrocarbons with one long *n*-alkyl substituent on a cyclopentane or cyclohexane ring constitute an important fraction of virgin naphtha. Little is known about the fate of such molecules in isomerization, hydrocracking, and catalytic dewaxing processes. Studies reported in literature most of the time deal with relatively small alicyclic hydrocarbon molecules containing 10 C atoms or less (1–4).

The reaction mechanisms of isomerization and hydrocracking of small alicyclic hydrocarbons on bifunctional zeolite-based hydrocracking catalysts such as acid Y zeolites loaded with platinum metal are well understood (3, 5–8). The conversion pathways can be rationalized assuming that the skeletal changes in the molecules occur while the molecules are activated and transformed into alkylcarbenium ions. According to the conventional bifunctional reaction mechanism, this activation is achieved through dehydrogenation followed by protonation of the double bond (9, 10). Skeletal isomerization of alkylcarbenium ions proceeds through cyclization of the molecule into a substituted corner protonated cycloalkane followed by ring opening (11, 12). In these cyclizations, three rings (corner protonated cyclopropanes, CPCP) are more important than larger rings (13). Two isomerization mechanisms are possible, denoted with A and B (11). In type A isomerizations, there is no change in the degree of branching. The degree of branching of the carbon skeleton is obtained by considering that a tertiary and a quaternary C atom introduce one and two branchings, respectively. In type B, the branching degree is either lowered or increased. Mechanistically, type B isomerizations involve *a corner-to-corner proton jump* on the ring of the cyclic intermediate, whereas such a jump is not required for type A (14).

Examples of reaction mechanisms of skeletal isomerization of alicyclic alkylcarbenium ions are provided in Fig. 1: (i) Positional shifts of alkyl substituents on a ring (**ex**ocyclic **a**lkyl **s**hifts) are of type A and will be denoted as A^{rex} (Fig. 1a). (ii) Elongation or shortening of existing side chains are another kind of type A reaction on the rings (**en**docyclic **a**lkyl **s**hifts) and are indicated with A^{ren} (Fig. 1b). In A^{rex} rearrangements, the ring size is not altered, while in A^{ren} conversions, the ring is contracted or expanded with one C atom. (iii) The generation of vanishing of a methylbranching on a ring is a type B isomerization (**r**ing **b**ranching, B^r). It results in contraction or expansion of the ring by one C atom (Fig. 1c). (iv) Similarly, new side chains on an alkyl substituent of the ring can be generated or eliminated by type B isomerization (**c**hain **b**ranching, B^c) (Fig. 1d), or branching positions on a chain can be altered via type A isomerizations (mechanism A^c) (Fig. 1e.)

In the bifunctional conversion of poly-alkylsubstituted cyclohexanes, the ring is preserved and the different methyl (ethyl, propyl) substituents on the ring are combined into one branched alkyl group via a combination of A^{rex} and A^c steps (1, 2). Upon cracking of the molecule, the bulky alkyl substituent is eliminated from the ring, explaining why this reaction is referred to as the *Paring* reaction (2).

In a previous publication (5), the isomerization of 1-cyclohexyloctane on a faujasite type hydrocracking catalyst was studied. A detailed reaction scheme of skeletal isomerization of this model molecule was established

0021-9517/98 $25.00

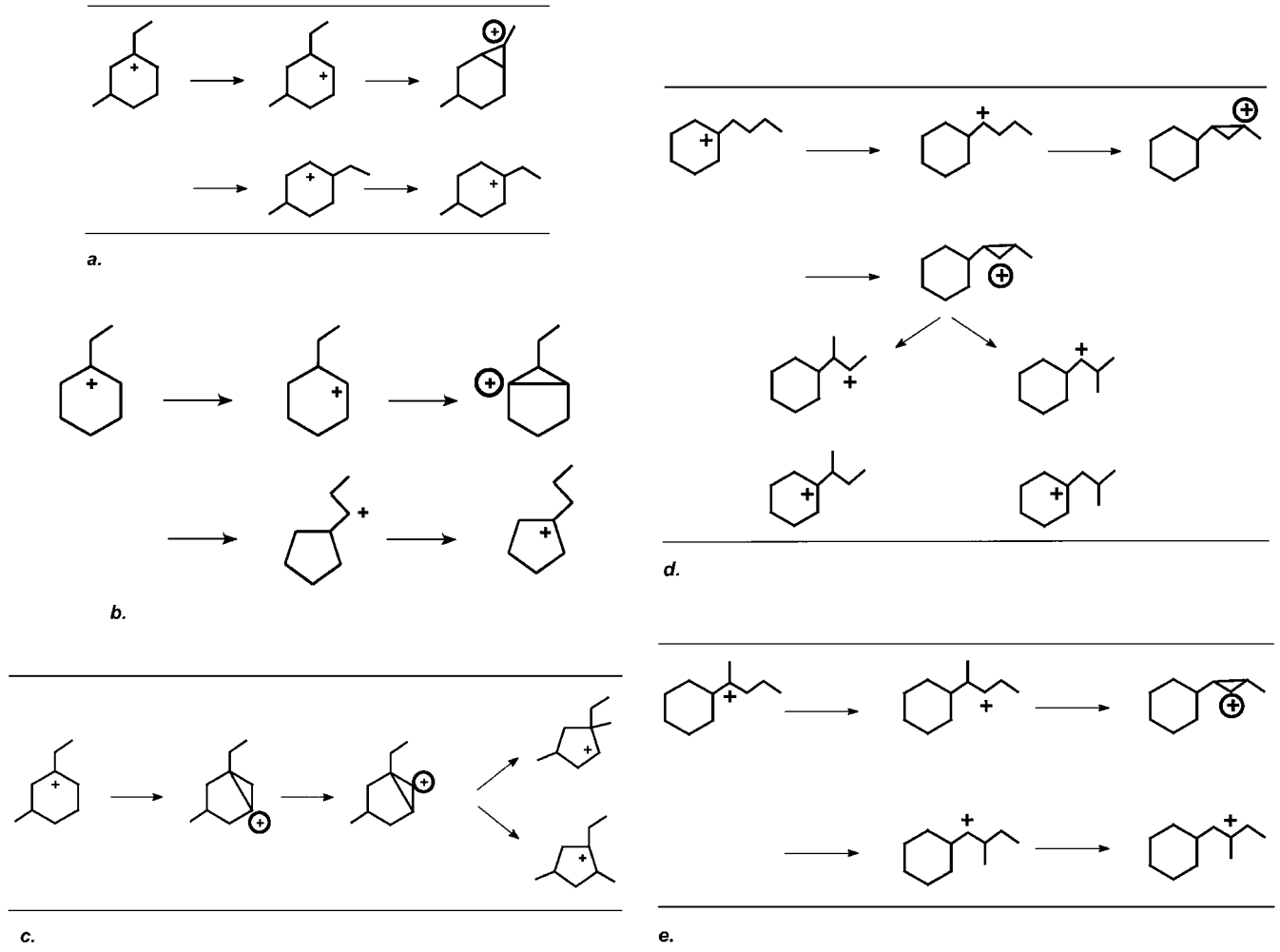

FIG. 1. Reaction mechanisms involved in the bifunctional conversion of alkylcycloalkanes: (a) exocyclic alkyl shift (A^{rex}); (b) endocyclic alkyl shift (A^{ren}); (c) ring branching (B^{r}); (d) chain branching (B^{c}); and (e) alkyl shift in side chain (A^{c}).

(Fig. 2). Typically, the degree of branching of this alicyclic hydrocarbon molecule is increased by a generation of branchings in the ring, rather than in the *n*-alkyl substituent (5). Subsequently, methyl branchings are transferred from ring to chain positions through A^{rex} and A^{c} mechanisms (Fig. 2) (5).

In the present study, a platinum-loaded ZSM-22 zeolite in its portonic form is used as a catalyst for converting 1-cyclohexyloctane. The ZSM-22 zeolite has the TON framework topology (15) and contains parallel, uniform tubular pores with the smallest pore cross-section diameters (0.55×0.45 nm) among the currently known tubular pore zeolites (15, 16). Isomerizations of long-chain *n*-alkanes on the Pt/H-ZSM-22 zeolite occur according to a very peculiar selectivity (17). A high selectivity for methyl branching at C_2 positions is encountered and explained via a branching mechanism, where part of the hydrocarbon molecule is sucked into a micropore of the zeolite crystal, while the branching is generated at the other end of the carbon chain positioned at the pore opening (17–20). Further multibranching involves a stretching of the hydrocarbon chain over the exterior crystal surface, allowing branchings to be generated at specific carbon atom positions where the hydrocarbon chain covers an opening to a pore (17). The favored isomers match their structures with the spacing of pore openings on the external surface of the ZSM-22 crystals according to a key–lock concept (17, 21). In this study, we were particularly interested in the conversion pathways of a probe molecule representing a combination of a long *n*-alkyl chain and a ring on the Pt/H-ZSM-22 catalyst.

EXPERIMENTAL

Catalytic Experiments

A sample of ZSM-22 zeolite was synthesized according to a recipe described in Ref. (22), method A. The Si/Al ratio in the framework, as determined by quantitative ^{27}Al

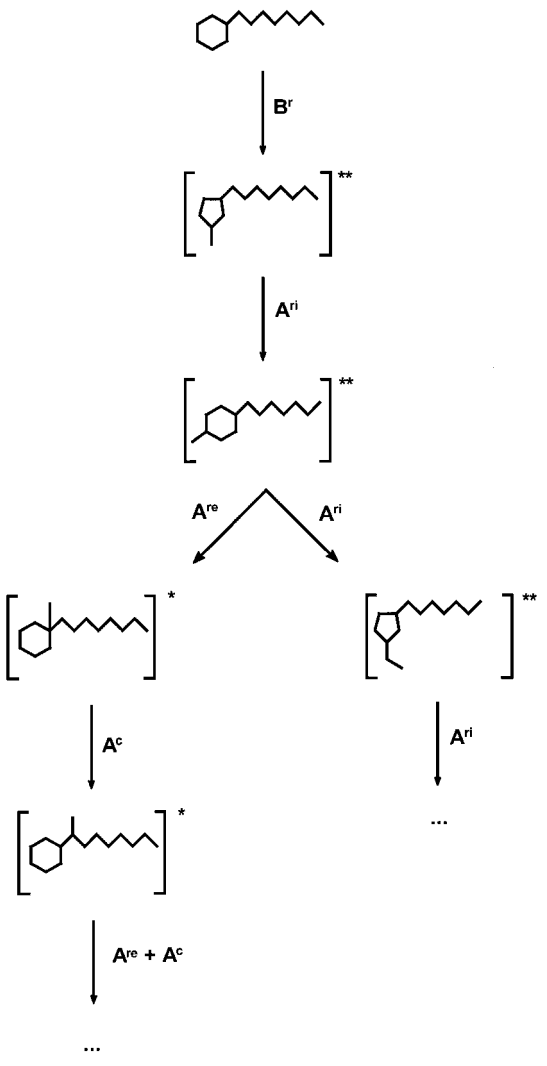

FIG. 2. Reaction pattern observed in the conversion of 1-cyclohexyloctane on a large pore Pt/H-Y zeolite catalyst (based on Ref. (5)). The square brackets and * indicate the occurrence of all positional and *cis–trans* isomers.

MAS NMR, amounts to 30. ZSM-22, calcined at 823 K, was cation-exchanged with ammonium and impregnated with an aqueous solution of $Pt(NH_3)_4Cl_2$ (incipient wetness technique) to obtain a Pt loading of 0.5 wt%. The zeolite powder was shaped into pellets with a diameter between 0.25 and 0.5 mm by compressing, crushing, and sieving. A 0.2-g sample of these pellets was charged into the stainless steel microreactor tube with internal diameter of 1 cm. Catalyst pretreatment comprised heating from 300 to 673 K under a stream of oxygen. After 1 h at 673 K, the bed was purged with nitrogen and contacted with hydrogen for another 1 h.

1-Phenyloctane (Janssen, 99%) was hydrogenated in a batch reactor on Pd/carbon black catalyst. The 1-cyclohexyloctane thus obtained was used as feed in the catalytic experiments.

The catalytic experiments were performed in a fixed-bed, continuous-flow microreactor with on-line GC analysis. The H_2 to 1-cyclohexyloctane molar ratio in the feed was 450 at a constant pressure at the reactor outlet of 0.45 MPa. The space time at the entrance of the reactor on hydrocarbon basis, W/F_0, amounted to 0.5 $kg \cdot h \cdot mol^{-1}$.

The GC-FID (HP5880A) and GC-MS (HP5998A) instruments were equipped with capillary columns (Chrompack) with CP-Sil-5CB stationary phase (film thickness of 1.31 μm), an internal diameter of 0.32 mm, a length of 120 m, and counting 300,000 theoretical plates. A substantial number of individual reaction products could be resolved and identified. Based on MS, the products could be classified according to their ring size and the number and type of alkyl substituents. Positional and *cis–trans* isomers of heptyl,methylcyclohexanes could be identified based on elution sequences of lighter methyl,alkyl-substituted cycloalkanes. The fraction of unidentified products was relatively small at low conversion (Fig. 3) and represents compounds with strongly overlapping or small chromatographic signals.

Molecular Modeling

Software running on a personal computer with a Pentium 133 processor was developed to calculate the adsorption potential of adsorbed molecules. A micropore fragment of a rigid SiO_2 polymorph with ZSM-22 structure was generated using the crystallographic data from Ref. (23). The framework fragment was made large enough to avoid boundary effects (362 oxygen atoms, three atomic layers around the pore). Geometry optimization of the hydrocarbon molecules was performed via HYPERChem V 3.0 for Windows. The molecules were optimized in an MM^+ force field in a vacuum until a RMS gradient (total energy gradient calculated as a root mean square gradient) of 4×10^{-5} $kJ \cdot mol^{-1}$ was reached. Successively, a steepest descent, Fletcher–Reeves and Newton–Raphson

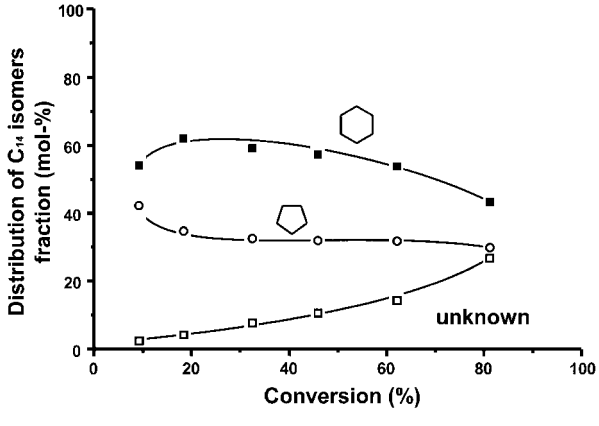

FIG. 3. Distribution of the isomer of the feed according to the type of ring system against 1-cyclohexyloctane conversion.

optimization algorithm was applied to reach the final optimized molecule.

The interaction potential $U_{L-J}(r_{ij})$ is calculated using a 12/6 Lennard–Jones potential function,

$$U_{L-J}(r_{ij}) = \sum_{\text{all } (ij) \text{ pairs}} \left(\frac{A_{ij}}{(r_{ij})^{12}} - \frac{B_{ij}}{(r_{ij})^{6}} \right), \qquad [1]$$

with r_{ij} denoting the distance between two interacting atomic (or molecular) centers and A_{ij} and B_{ij}, the repulsive and dispersive interaction parameters, respectively. Values for A_{ij} and B_{ij} for oxygen–hydrogen and oxygen–carbon interactions valid for silicate frameworks were retrieved from Ref. (24). For the position optimization of hydrocarbons in the ZSM-22 micropore the following procedure has been applied. First, the hydrocarbon was docked manually in the center of the micropore. Then, the position with lowest potential was searched via a three-dimensional rotation–translation procedure using a steepest descent algorithm. In order to avoid local minima, the translation and rotation step sizes were increased again whenever the hydrocarbon had reached an optimum.

RESULTS AND DISCUSSION

In the chromatograms of the reaction products from 1-cyclohexyloctane conversion on Pt/H-ZSM-22, the C_{14} fraction, including the feed, was clearly separated from the products containing fewer carbon atoms. The conversion of the feed and the isomerization and cracking yields obtained at increasing reaction temperatures are shown in Fig. 4. Isomerization and cracking are consecutive reactions. The fraction of unidentified C_{14} products is relatively small, but increases with conversion (Fig. 3). Substituted cyclohexanes are more abundant than cyclopentanes (Fig. 3).

The identified C_{14} isomers contain a 5- or a 6-ring and have either two *n*-alkyl-substituents or one isoalkyl substituent (Fig. 5). The evolution with increasing conversion of the distribution of these two groups of isomers shown in Fig. 5 must be interpreted with some caution in view of the increasing fraction of unidentified products (Fig. 3). Di-*n*-alkylsubstituted cyclopentanes and cyclohexanes are the main skeletal isomerization products obtained (Fig. 5).

Specific cyclopentanes and hexanes with two *n*-alkyl substituents are formed, namely cyclopentanes with ethyl + heptyl, propyl + hexyl, and butyl + pentyl substituents and cyclohexanes with methyl + heptyl and ethyl + hexyl substituents, respectively (Fig. 6). The possibility that molecules with other substituent combinations are formed in smaller quantities cannot be precluded, but in that instance they could not be analyzed and are contained in the unknown product fraction.

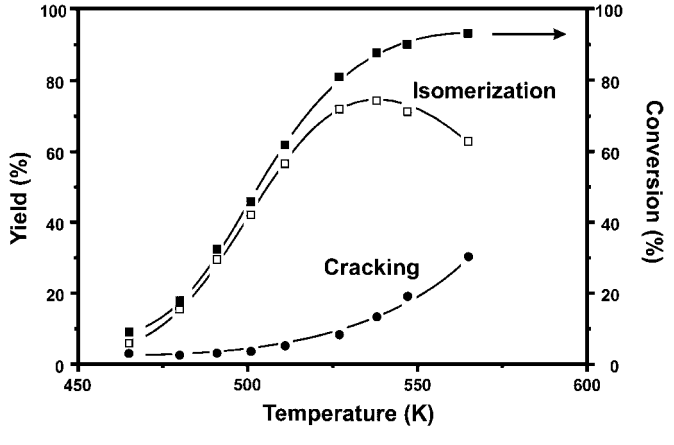

FIG. 4. Conversion, isomerization, and cracking yield in the reaction of 1-cyclohexyloctane on Pt/H-ZSM-22 zeolite.

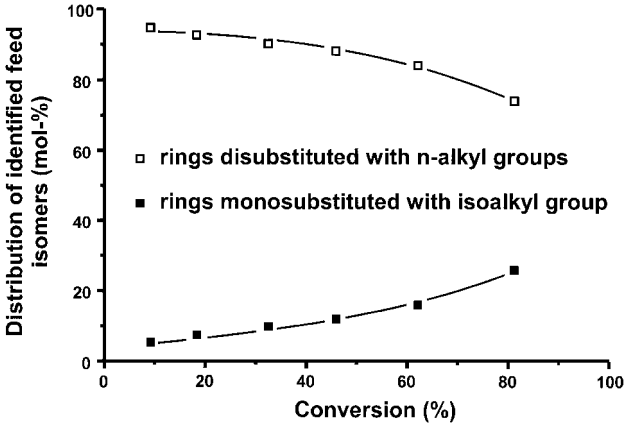

FIG. 5. Distribution of the isomers of the feed according to the number of ring substituents against 1-cyclohexyloctane conversion.

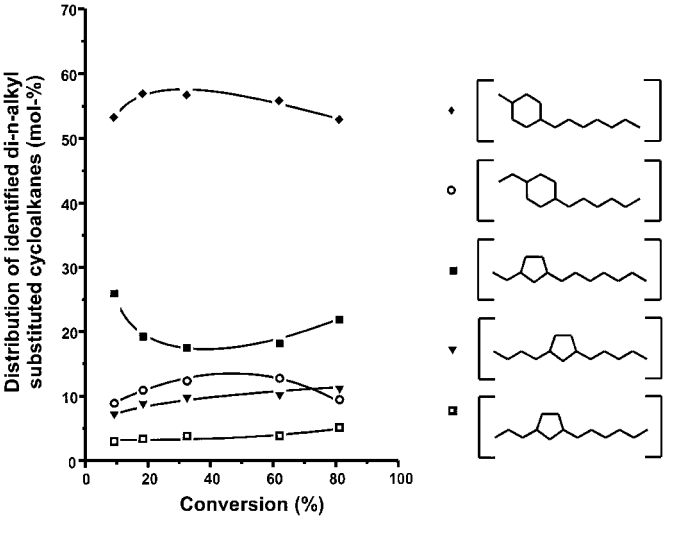

FIG. 6. Distribution of identified di-*n*-alkyl-substituted cycloalkane feed isomers against conversion (a limited number of positional and *cis–trans* isomers).

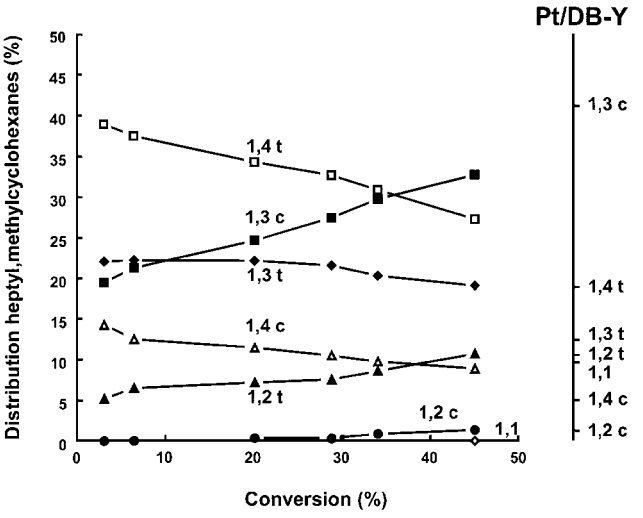

FIG. 7. Distribution of positional and *cis–trans* heptyl,methyl-substituted cyclohexane feed isomers against conversion. Values at the right-hand side of the graph indicate the equilibrium distribution as observed on a FAU-type Pt/H-Y zeolite (5).

Heptyl,methylcyclohexanes are the most important skeletal isomers (Fig. 6). The evolution with conversion of their distribution is shown in Fig. 7. On Pt/H-ZSM-22, the 1,1′-disubstituted isomer is not formed. The formation of 1,3c, 1,2t, and 1,2c is kinetically suppressed in favor of the 1,4t 1,3t, and 1,4c substitution (Fig. 7).

Via the molecular modeling, the origin of this peculiar selectivity could be elucidated. Owing to the presence of the cyclohexane ring, none of the heptyl,methylcyclohexanes was able to attain a favorable potential inside the micropores. The lowest potential is reached after plugging of the heptyl group into the micropore until the cyclohexane moiety hits the window of the pore (Table 1). Such an interaction resembles a cork on a bottle. For the 1,1′- and 1-*t*-4-heptyl,methylcyclohexane isomers, the optimized positions are shown in Fig. 8. The results from the potential calculations for the different isomers are listed in Table 1. The potential is largely dependent on the position of the methyl substituent on the ring. The closer the two alkyl groups, the higher the potential value.

TABLE 1

Interaction Potential of 1-Cyclohexyloctane, 1-Cyclopentylnonane, and Positional and *cis–trans* Heptyl,methylcyclohexane Isomers Position Optimized in a Pore Mouth of ZSM-22

Isomer	Interaction potential ($kJ \cdot mol^{-1}$)
1-Cyclohexyloctane	−129
1-Cyclopentylnonane	−134
1-*t*-4-Heptyl,methylcyclohexane	−146
1-*t*-3-Heptyl,methylcyclohexane	−141
1-*c*-3-Heptyl,methylcyclohexane	−133
1-*c*-4-Heptyl,methylcyclohexane	−129
1-*t*-2-Heptyl,methylcyclohexane	−110
1-*c*-2-Heptyl,methylcyclohexane	−106
1,1′-Heptyl,methylcyclohexane	−105

The order of formation of the individual heptyl, methylcyclohexane isomers at low feed conversion levels (Fig. 7) follows the order of the potentials of these molecules (Table 1). Apparently, the selectivity evolves from the stereochemistry of the pore mouths of the ZSM-22 zeolite crystals.

In contrast to on a Pt/H-Y catalyst (5), on Pt/H-ZSM-22 one specific isomer is selectively formed in the product fractions of di-*n*-alkyl-substituted cyclopentanes and hexanes with both substituents larger than a methyl group. The GC-MS analytical technique did not allow us to determine the relative positions of the alkyl groups on the ring, nor whether they were *cis* or *trans* isomers. For the di-*n*-alkylsubstituted cyclohexanes, it can be speculated that the preferred isomers are 1-($C_{8-x}H_{17-2x}$)-*t*-4-(C_xH_{2x-1})-cyclohexanes ($1 < x \leq 4$), by analogy with the heptyl,methylcyclohexanes.

On Pt/H-Y (5), branchings are generated on the ring (B^r) and transferred subsequently to the alkyl substituents through a combination of A^{re} and A^c (Fig. 2). The 1,1′-alkyl,methylcycloalkanes are key intermediates in this mechanism (Fig. 2) (5). As a result, initially the methyl group on the alkyl side chain is positioned close to the ring. Via subsequent type A isomerizations, the methyl branching is shifted to C-atom positions more distant from the ring (5). In the reaction products obtained in the present work using Pt/H-ZSM-22 catalyst, a substantial number of 1-cyclopentylmethyloctanes could be identified and quantified. The evolution of the distribution of this fraction with feed conversion is presented in Fig. 9. In this case, the methyl side chain occurs preferentially at C-atom positions remote from the ring (Fig. 9). These isomers seem to originate from a direct branching-type rearrangement of the *n*-alkyl substituent (B^c mechanism). On Pt/H-ZSM-22, the formation of 1,1′-di-*n*-alkyl-substituted rings is suppressed (cf. 1,1′-isomers in the heptyl,methylcyclohexane fraction, Fig. 7). Furthermore, a ring-to-chain transfer mechanism of methyl branchings would imply that branching positions close to the ring are favored initially, which is not observed experimentally (Fig. 9). Probably, the 1-cyclopentylmethyloctanes arise from the following sequence of transformations. First, there is an elongation of the alkyl side chain with concomitant ring contraction yielding 1-cyclopentylnonane. This transformation is facilitated as it leads to a lower potential (Table 1). Subsequently, a methyl branching is generated in the nonyl group. The methyl branching cannot occur while the molecule is adsorbed according to the plugging mode. The alternative adsorption mode is with the cyclohexane ring adsorbed on the window of one pore, while the *n*-alkyl chain is entering

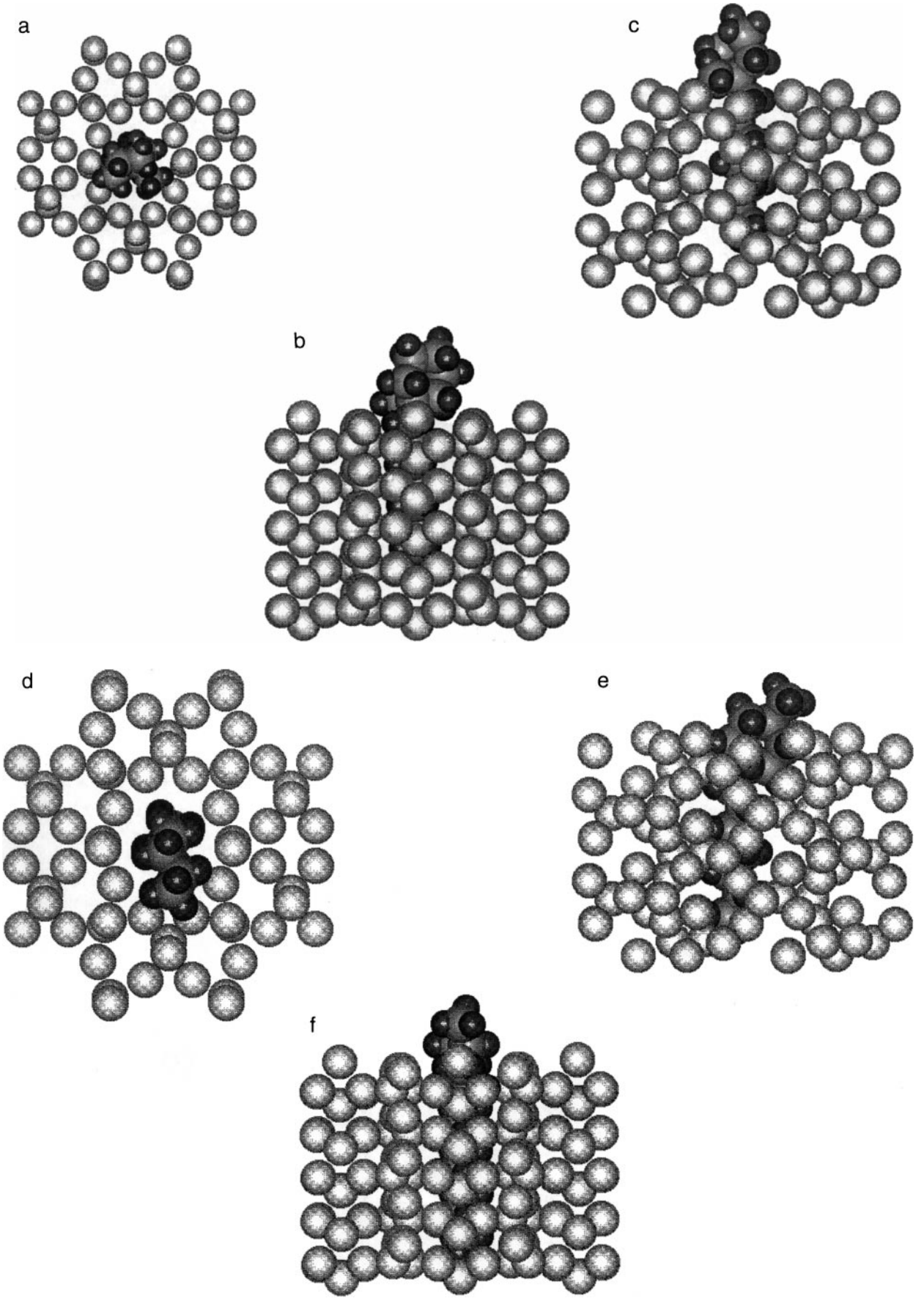

FIG. 8. Favorable adsorption loci for 1,1′- (a–c) and 1-*t*-4-heptyl,methylcyclohexane (d–f) isomers in the pore mouth of ZSM-22. (a) and (d) view along the (001) direction, (b) and (f) view along the (110) direction, and (c) and (e) view along the (100) direction.

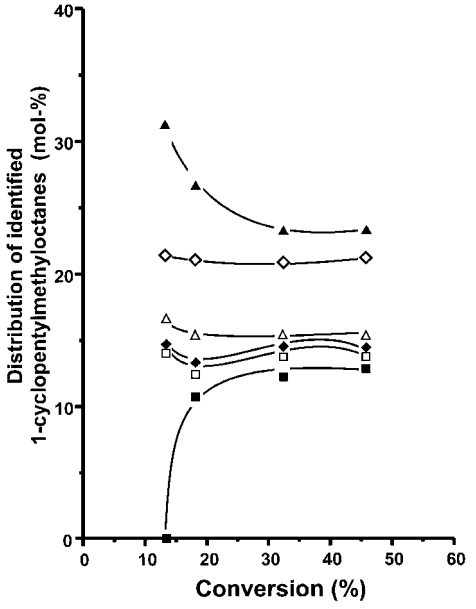

FIG. 9. Distribution of identified dibranched monoalkyl-substituted cyclopentanes against conversion: (■) 2-cyclopentylnonane, (□) 1-cyclopentyl-2-methyloctane, (◆) 1-cyclopentyl-3-methyloctane, (◇) 1-cyclopentyl-4-methyloctane, (△) 1-cyclopentyl-5-methyloctane, and (▲) 1-cyclopentyl-7-methyloctane.

a second neighboring pore mouth. The preferred methyl branching positions correspond to the ones facing a pore mouth when the molecule is stretched over the external zeolite surface, with the ring positioned in front of a hole (Fig. 10). In this way, the direct chain branching can be considered a special case of key–lock catalysis.

The key–lock adsorption mode explains also how side-chain elongations/shortenings and ring contractions/expansions are likely to occur without penetration of the ring into the micropores. Part of the long *n*-alkyl chain is stretched over the bridge of zeolite framework spanning two pore mouths (Scheme 1). In such a position, the generation of a side chain and its subsequent elongation correspond to a transfer of methylene carbons from one pore to another. This can be considered a shifting of a cycloalkane ring along a molecular carbon wire.

Finally, the proposed model for the conversion of long-chain alkylcycloalkanes on Pt/H-ZSM-22 also allows us to rationalize the high maximum yield of isomerization observed with this catalyst (76%) (Fig. 4). This is much higher than that with Pt/H-Y zeolite (40%) (5). The lower tendency to cracking on Pt/H-ZSM-22 can be readily explained by the suppression of the "paring" reaction in which the formation of 1,1′-dialkylcycloalkane intermediates is required.

CONCLUSIONS

A detailed analysis of particular reaction product fractions reveals that Pt/H-ZSM-22 exhibits distinctly different reaction selectivities in the conversion of 1-cyclohexyloctane compared to a large pore Pt/H-Y zeolite catalyst. The formation of 1,1′-di-*n*-alkyl substituents is suppressed. These are key intermediates in ring-to-chain transfers of branchings and in the paring reaction. It explains why the skeletal isomers have little tendency to cracking on Pt/H-ZSM-22. Potential calculations suggest that the cyclic moiety of the molecule does not cross the pore window. In

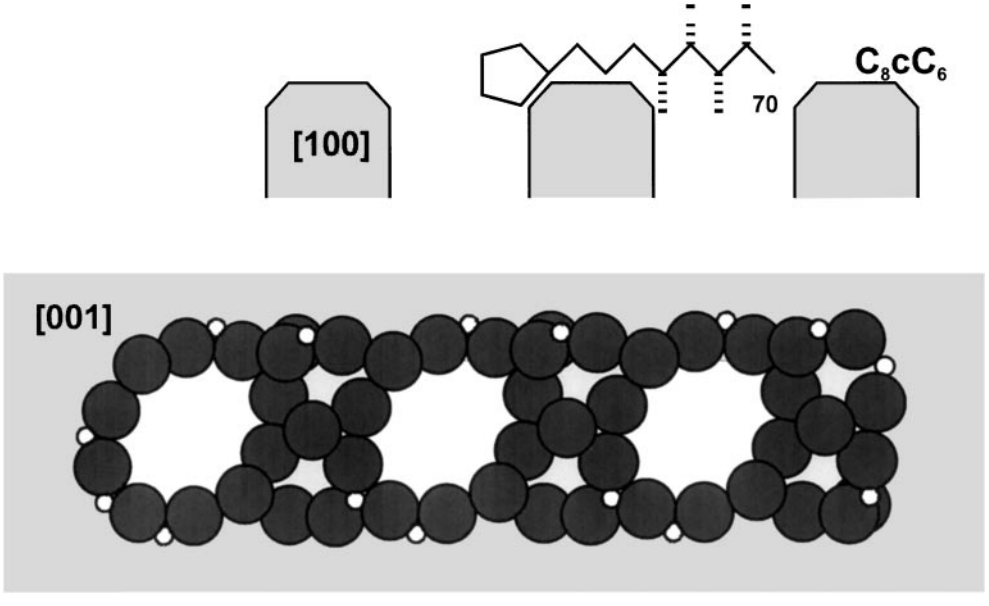

FIG. 10. Schematic representation of the key–lock adsorption mode invoked to rationalize the 1-cyclopentylmethyloctane isomer distributions observed on Pt/H-ZSM-22 in the conversion of 1-cyclohexyloctane.

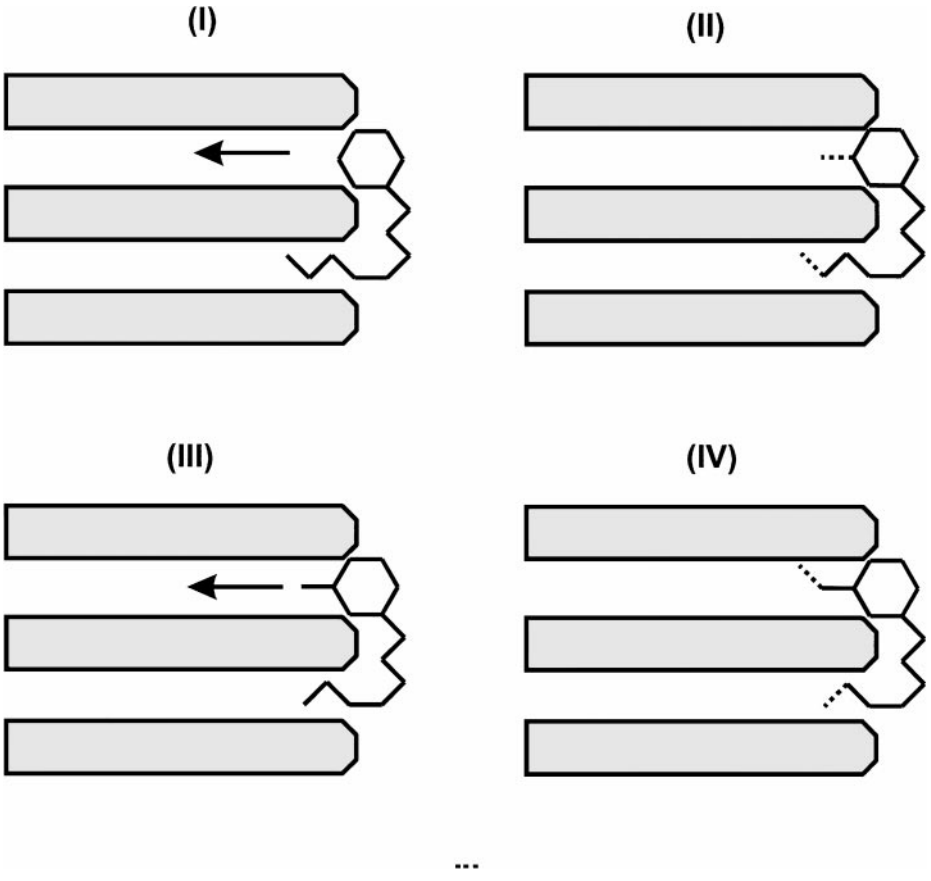

SCHEME 1

favored adsorption sites, the *n*-alkyl substituents on the ring penetrate into a micropore. The observed product patterns can be explained via pore mouth and molecular plugging mechanisms.

ACKNOWLEDGMENTS

W.S. and E.F. are indebted to the IWT for a research fellowship. J.A.M. acknowledges FWO for a research position. This work has been sponsored by the Belgium Government within the frame of an IUAP Center of Excellence Program and by the Flemish Government in the frame of a Concerted Research Action (GOA).

REFERENCES

1. Sullivan, R. F., Egan, C. J., Langlois, G. E., and Sieg, R. P., *J. Am. Chem. Soc.* **83**, 1156 (1961).
2. Egan, C. J., Langlois, G. E., and White, R. J., *J. Am. Chem. Soc.* **84**, 1204 (1962).
3. Jacobs, P. A., Tielen, M., Martens, J. A., and Beyer, H. K., *J. Mol. Catal.* **27**, 11 (1984).
4. Weitkamp, J., Ernst, S., and Kumar, R., *Appl. Catal.* **27**, 207 (1986).
5. Souverijns, W., Parton, R., Martens, J. A., Froment, G. F., and Jacobs, P. A., *Catal. Lett.* **37**, 207 (1996).
6. Weitkamp, J., Jacobs, P. A., and Ernst, S., *in* "Structure and Reactivity of Modified Zeolites" (P. A. Jacobs, N. I., Jaeger, P. Jiru, V. B. Kazansky, and G. Schulz-Ekloff, Eds.), p. 279, Elsevier, Amsterdam, 1984. [Stud. Surf. Sci. Catal., Vol. 18]
7. Jacobs, P. A., Tielen, M., and Sosa, R. C., *in* "Structure and Reactivity of Modified Zeolites" (P. A., Jacobs, N. I. Jaeger, P. Jiru, V. B. Kazansky, and G. Schulz-Ekloff, Eds.), p. 175, Elsevier, Amsterdam, 1984. [Stud. Surf. Sci. Catal., Vol. 18]
8. Weitkamp, J., Ernst, S., and Chen, C. Y., *in* "Zeolites: Facts, Figures, Future" (P. A. Jacobs and R. A. Van Santen, Eds.), p. 1115, Elsevier, Amsterdam, 1989. [Stud. Surf. Sci. Catal., Vol. 49B]
9. Coonradt, M. L., and Garwood, W. E., *Ind. Eng. Chem. Prod. Res. Dev.* **3**, 38 (1964).
10. Weisz, P. B., *Adv. Catal.* **13**, 137 (1962).
11. Vogel, P., *in* "Carbocation Chemistry," Studies in Organic Chemistry 21, p. 323, Elsevier, Amsterdam, 1985.
12. Weitkamp, J., *Ind. Eng. Chem. Prod. Res. Dev.* **21**, 550 (1982).
13. Martens, J. A., and Jacobs, P. A., *J. Catal.* **124**, 357 (1990).
14. Martens, J. A., and Jacobs, P. A., *in* "Theoretical Aspects of Heterogeneous Catalysis" (J. B. Moffat, Ed.), p. 52, Van Nostrand Reinhold, 1990.
15. Barri, S. A. I., Smith, G. W., White, D., and Young, D., *Nature* **312**, 534 (1984).
16. Meier, W. M., and Olson, D. H., "Atlas of Zeolite Structure Types," 4th ed., *Zeolites*, Vol. 17, p. 1, Kluwer Acad., Dordrecht, 1996. [NATO ASI Ser. E]
17. Martens, J. A., Souverijns, W., Verrelst, W., Parton, R., Froment, G. F., and Jacobs, P. A., *Angew. Chem. Int. Ed. Engl.* **34**(22), 2528 (1995).
18. Ernst, S., Kokotailo, G. T., Kumar, R., and Weitkamp, J., *in* "Proceedings from the 9th International Zeolite Conference" (R. von Ballmoos,

J. B. Higgins, and M. M. J. Treacy, Eds.), Vol. 1, p. 287, Butterworth-Heinemann, Boston, 1993.
19. Ernst, S., Weitkamp, J., Martens, J. A., and Jacobs, P. A., *Appl. Catal.* **48**, 137 (1989).
20. Martens, J. A., Parton, R., Uytterhoeven, L., Jacobs, P. A., and Froment, G. F., *Appl. Catal.* **76**, 95 (1991).
21. Souverijns, W., Martens, J. A., Uytterhoeven, L., Froment, G. F., and Jacobs, P. A., *in* "Progress in Zeolite and Microporous Materials" (H. Chon, S.-K. Kim, and Y. S. Uh, Eds.), p. 1285, Elsevier, Amsterdam. [Stud. Surf. Sci. Catal., Vol. 105]
22. Olson, D. H., Calvert, C. J., and Valyocsik, E. W., EPA 102,716 assigned to Mobil Oil, 1984.
23. Kokotailo, G. T., Schlenker, J. L., Dwyer, F. G., and Valyocsik, E. W., *Zeolites* **5**, 349 (1985).
24. Picket, S. D., Nowak, A. K., Thomas, J. M., and Cheetham, A. K., *Zeolites* **9**, 123 (1989).